NeuroImage 152 (2017) 639–646

Contents lists available at ScienceDirect

NeuroImage

journal homepage: www.elsevier.com/locate/neuroimage

The epidemic spreading model and the direction of information flow in brain networks

J. Meier[a,*], X. Zhou[a], A. Hillebrand[b], P. Tewarie[c,d], C.J. Stam[e], P. Van Mieghem[a]

[a] Faculty of Electrical Engineering, Mathematics and Computer Science, Delft University of Technology, P.O Box 5031, 2600 GA Delft, The Netherlands
[b] Department of Clinical Neurophysiology and Magnetoencephalography Center, VU University Medical Centre, Amsterdam, The Netherlands
[c] Department of Neurology, VU University Medical Center, Amsterdam, The Netherlands
[d] Sir Peter Mansfield Imaging Centre, School of Physics and Astronomy, University of Nottingham, University Park, Nottingham, United Kingdom
[e] Department of Clinical Neurophysiology, VU University Medical Center, Amsterdam, The Netherlands

ARTICLE INFO

Keywords:
Brain networks
Effective connectivity
SIS model
Transfer entropy
Information flow
Global patterns

ABSTRACT

The interplay between structural connections and emerging information flow in the human brain remains an open research problem. A recent study observed global patterns of directional information flow in empirical data using the measure of transfer entropy. For higher frequency bands, the overall direction of information flow was from posterior to anterior regions whereas an anterior-to-posterior pattern was observed in lower frequency bands. In this study, we applied a simple Susceptible-Infected-Susceptible (SIS) epidemic spreading model on the human connectome with the aim to reveal the topological properties of the structural network that give rise to these global patterns. We found that direct structural connections induced higher transfer entropy between two brain regions and that transfer entropy decreased with increasing distance between nodes (in terms of hops in the structural network). Applying the SIS model, we were able to confirm the empirically observed opposite information flow patterns and posterior hubs in the structural network seem to play a dominant role in the network dynamics. For small time scales, when these hubs acted as strong receivers of information, the global pattern of information flow was in the posterior-to-anterior direction and in the opposite direction when they were strong senders. Our analysis suggests that these global patterns of directional information flow are the result of an unequal spatial distribution of the structural degree between posterior and anterior regions and their directions seem to be linked to different time scales of the spreading process.

Introduction

Analyzing the human brain as a network led to the discovery of many interesting properties (Stam, 2014; Stam and Van Straaten, 2012; Bullmore and Sporns, 2012). However, different measurement techniques capture different aspects of brain networks. Techniques such as diffusion tensor imaging (DTI) allow for the reconstruction of the structural brain network, which consists of a map of anatomical connections between brain regions. Functional imaging techniques, such as magneto-/electro-encephalography (MEG/EEG) and functional magnetic resonance imaging (fMRI), measure, either directly or indirectly, the activity of brain regions, from which functional brain networks can be reconstructed. Based on the brain regions' time series of activation we can extract two types of connectivity information: Functional connectivity refers to the existence of a statistical relationship between the activation time series, whereas effective connectivity captures the causal effect of one region's activity to the other regions' activities (Aertsen et al., 1989; Friston, 1994). While most studies have analyzed functional connectivity, recent approaches have focused on effective connectivity to gain knowledge about directionality (Hillebrand et al., 2016; Moon et al., 2015; Stam and van Straaten, 2012). Patients suffering from brain disorders often have altered structural brain networks (Crossley et al., 2014). In order to understand how these structural changes influence changes in the functional networks, we need to reveal the properties of the underlying connectome that facilitate the information flow and its direction in the functional networks.

The measure of transfer entropy (TE) has been used for MEG and EEG data for the estimation of effective connectivity (Schreiber, 2000). Transfer entropy from node i to node j measures how much better a prediction of a next value of j becomes when we not only include the previous value of j but also the previous value of i. In the sense of

* Corresponding author.
E-mail addresses: j.m.meier@tudelft.nl (J. Meier), c.xyzhou@outlook.com (X. Zhou), a.hillebrand@vumc.nl (A. Hillebrand), prejaas.tewarie@nottingham.ac.uk (P. Tewarie), cj.stam@vumc.nl (C.J. Stam), p.f.a.vanmieghem@tudelft.nl (P. Van Mieghem).

http://dx.doi.org/10.1016/j.neuroimage.2017.02.007
Received 7 November 2016; Accepted 3 February 2017
Available online 05 February 2017
1053-8119/

Wiener's principle (Wiener, 1956), transfer entropy can be interpreted as the causal influence of one brain region on another. Recently, the measure of transfer entropy has been expanded to a measure for phase-based connectivity, the so-called Phase Transfer Entropy (Paluš and Stefanovska, 2003; Lobier et al., 2014). By applying the Phase Transfer Entropy, Hillebrand et al. (2016) recently found a surprisingly consistent global spreading pattern from posterior to anterior brain regions in empirical MEG data in the higher frequency bands (*alpha1*, *alpha2*, and *beta* band) and a mirrored information flow from anterior to posterior regions in the *theta* band, where the latter has also been observed in EEG data (Dauwan et al., 2016). The origin of these global patterns is still unclear. Hillebrand et al. (2016) hypothesized that this global direction of information flow could be driven by strong hub connections in the posterior regions possessing the highest levels of neuronal activity in the network during the resting-state (de Haan et al., 2012; Moon et al., 2015).

Recent studies have shown that simple models of activity spread can contribute to our understanding of brain dynamics (Abdelnour et al., 2014; Deco et al., 2012). For example, Mišić et al. (2015) applied a simple deterministic cascade model and discovered that hubs and the shortest paths of the structural brain network have a high influence on the efficiency of spreading dynamics. Even though those simple models ignore microscopic details of the spreading process, the scarcity of parameters simplifies the exposure of underlying general principles. Further, there is evidence that the brain operates near a critical phase transition (Tewarie et al., 2016; Haimovici et al., 2013; Yu et al., 2013; Rubinov et al., 2011). It is known from statistical physics that the details of the applied model become irrelevant near such a transition. This vicinity of a phase transition could explain why simple models (Deco et al., 2012; Haimovici et al., 2013) have been successful in capturing more complicated model findings (Honey et al., 2007, 2009).

A simple epidemic process often approximates empirical spreading processes on networks for various applications, e.g. information propagation and gossip spreading in social networks (Pastor-Satorras et al., 2015). The Susceptible-Infected-Susceptible (SIS) epidemic is one of the simplest models of an epidemic. In an SIS epidemic process, a node can be in two states, either infected or susceptible (and can be infected by its infected neighbors). The advantages of the epidemic spreading model are that the effective spreading rate τ is the only a-priori chosen parameter and that we can also study the model analytically. A previous study (Stam et al., 2016) applied a discrete-time epidemic process on the structural brain network and identified the structural degree product as a driving force for the effective connectivity between two nodes. In the case of the functional brain network, brain regions can be activated (infected) and spread this activation to their anatomically neighboring excitable (susceptible) regions. Applying the well-developed theory of epidemics may lead to a better understanding of the activity spreading in the brain and in particular reveal the structural properties that drive the global spreading dynamics.

The SIS process can analytically be described as a continuous-time Markov chain with 2^N states where N is the number of nodes in the network. The embedded Markov chain approximates the continuous-time SIS process as a discrete-time process and contains the transition probabilities but no longer the precise timing of the events (Van Mieghem, 2014b). For this study, we simulated an epidemic spreading process on the structural brain network in a continuous-time framework since we were interested in the smaller time-scale dynamics (see Fig. 1; Van Mieghem, 2014b). We used the transfer entropy (instead of the Phase Transfer Entropy) for the estimation of pairwise directed interactions since the SIS model generates binary time series.

The aim of this paper was to elucidate the topological properties of the structural brain network that give rise to the empirically observed effective connectivity patterns in functional brain networks. To this end, time series were generated by applying a continuous-time SIS model on a human connectome, following which effective connectivity

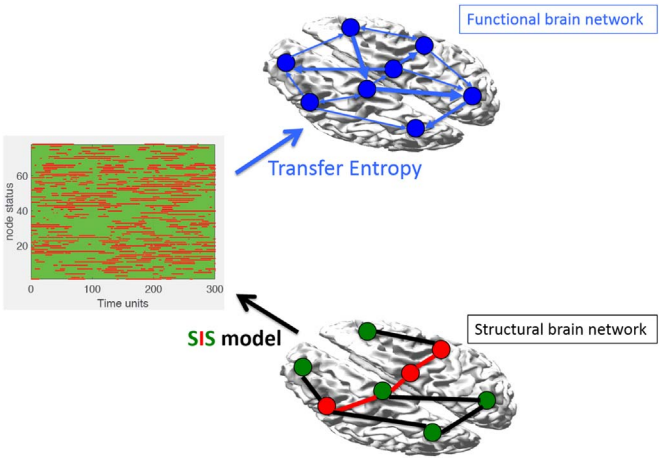

Fig. 1. Schematic overview of performed modelling. We ran a Susceptible-Infected-Susceptible (SIS) process on the underlying structural brain network. Based on the activation time series of the nodes (see left panel, red represents the activated state and green the excitable state), we calculated all pairwise transfer entropies to construct a network of the same nodes but with the link weights representing the functional interactions between node activities.

was estimated using pairwise transfer entropies for different time delays. Because previous studies (Stam et al., 2016; Mišić et al., 2015; Tewarie et al., 2014) and analytic reasoning (see Appendix E in Supplementary material) identified the degree as a driving force behind spreading dynamics, we directed a special focus on the relationship between the structural degree and the outcome of the SIS spreading process.

Methods

Structural network

For the structural network, we used a literature-based DTI network from a previous study based on 80 healthy subjects (for details see Gong et al. (2009)), where a node corresponds to a cortical region in the automated anatomical labeling (AAL) atlas (Tzourio-Mazoyer et al., 2002). In short, every two cortical regions from the 78 AAL atlas regions were considered to be connected if the end points of two white matter tracts were located in these regions (Gong et al., 2009). Via a non-parametric sign test only the significant links were included in the group-averaged structural connectivity matrix. This processing resulted in a binary connectivity matrix for the structural brain network, which we will further refer to as the structural adjacency matrix A.

SIS process

In an SIS epidemic process on an undirected and unweighted graph G with N nodes and L links, the state of a node i at time t is specified by a Bernoulli random variable $X_i(t) \in \{0, 1\}$: $X_i(t) = 0$ for an excitable node and $X_i(t) = 1$ for an activated node. Here, we have replaced the states 'susceptible' and 'infected' from classic epidemic theory with 'excitable' and 'activated' to indicate the status of a brain region. Only an active node can activate its direct neighbors that are still excitable. We assume that the infection (activation) process and the curing process (change to excitable status) are Poissonian with rates β (infection rate) and δ (curing rate), respectively (Van Mieghem, 2014b). The infection and curing process are independent of each other. The continuous-time SIS model is defined by the differential equation for the expected status of any node j, $E[X_j]$,

$$\frac{dE[X_j]}{dt} = E\left[-\delta X_j + (1 - X_j)\beta \sum_{k=1}^{N} a_{kj} X_k\right], \tag{1}$$

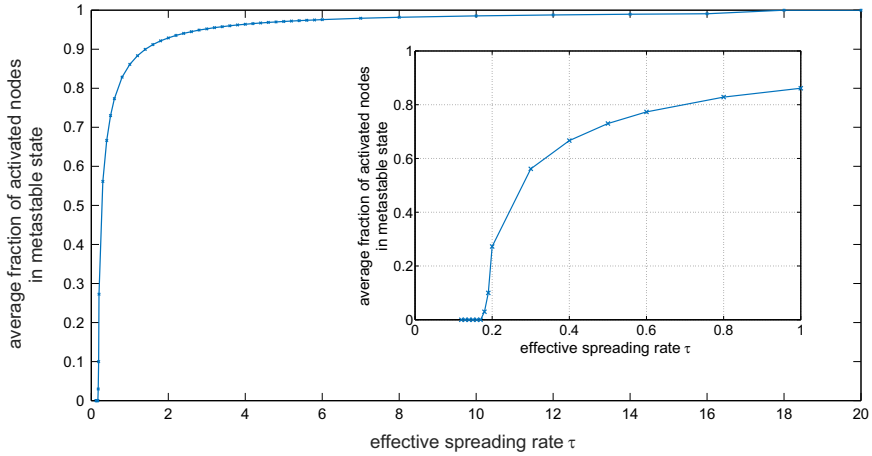

Fig. 2. Average fraction of activated nodes. Average fraction of activated nodes in metastable state for different effective infection rates τ. The smaller graphic is a zoomed-in plot for smaller values of τ.

where $\sum_{k=1}^{N} a_{kj} X_k$ counts the number of activated neighbors of node j. The effective infection rate is denoted by $\tau = \beta/\delta$.

Details of the simulation

As mentioned in the introduction, there is evidence that the brain operates with its dynamics near a critical phase transition (Haimovici et al., 2013; Rubinov et al., 2011; Yu et al., 2013). As in Stam et al. (2016), we chose β and δ such that the SIS dynamics are slightly above the critical epidemic threshold τ_c which we verified with continuous-time simulations (Fig. 2). We used the continuous-time simulator SIS simulator (SISS) (van de Bovenkamp, 2015) to simulate an SIS-epidemic on the structural network with $\beta = 0.1$ and $\delta = 0.5$ (Stam et al., 2016) resulting in an effective spreading rate $\tau = \beta/\delta = 0.2$. For each simulation run, we initially activated 15 nodes at random, which is approximately 20% of the whole network, to enable a comparison with previous results (Stam et al., 2016). Initially infecting 15 nodes also ensures that the probability for the activity-spread to die out is nearly zero (Liu and Van Mieghem, 2016a; see Fig. A.1 in Supplementary material).

We ran a simulation of 4096 time units (Stam et al., 2016). We applied 0.1 time units as a sample interval resulting in 40960 time points for one simulation, forming for each node an activation time series of zeros (node is not activated at time instance t) and ones (node is activated at time instance t) (for an example of an activation time series see Fig. 1). To focus on the metastable (quasi-stationary) state (Van Mieghem, 2014b), we disregarded the initial phase of the spreading process by calculating all our results based on the second half of the simulation time (from 2048 to 4096 time units). There exists no analytic reasoning for the metastable state of an epidemic spreading process yet (Cator and van Mieghem, 2013; Liu and van Mieghem, in press) but based on our simulation results we can conclude that extracting the second half of the simulation time assures the exclusion of the initial phase (see Fig. A.2 in Supplementary material). All presented results were averaged over 100 simulation runs.

Transfer entropy

In order to capture the delayed influence, we calculated for every node pair i and j the transfer entropy (TE) from node i to node j over the whole simulation time series as

$$TE_{i\to j}(h) = \sum_{k,l,m=\{0,1\}} \Pr[X_j(t+h)=k, X_j(t)=l, X_i(t)=m] \cdot \log\left(\frac{\Pr[X_j(t+h)=k | X_j(t)=l, X_i(t)=m]}{\Pr[X_j(t+h)=k | X_j(t)=l]}\right) \quad (2)$$

for a certain time delay h. Transfer entropy can be interpreted as a delayed correlation measure that is corrected for auto-correlation, which we can employ for analytic derivations (see Appendix D and Appendix E in Supplementary material). Similar to Hillebrand et al. (2016), we defined the directed transfer entropy (dTE) from node i to node j as

$$dTE_{i\to j}(h) = \frac{TE_{i\to j}(h)}{TE_{i\to j}(h) + TE_{j\to i}(h)}, \quad (3)$$

which quantifies the preferred direction of flow. Since the transfer entropy can only take positive values, the directed transfer entropy measure is well-defined and ranges from 0 to 1. If the preferred flow of information is from node i to node j, then $0.5 < dTE < 1$, else $0 < dTE < 0.5$. For every node, we calculated the average value of the directed transfer entropy from this node to all other nodes in the network. If this averaged directed transfer entropy for node i was larger (smaller) than 0.5, then node i is a preferred sender (receiver) of information. In order to quantify the global pattern of information flow, we calculated a posterior-anterior (PA) index

$$PA = \overline{dTE}_{posterior} - \overline{dTE}_{anterior},$$

where $\overline{dTE}$ denotes the average over the directed transfer entropy values of all posterior and anterior regions, respectively (Hillebrand et al., 2016). Thus, a positive posterior-anterior value indicates a posterior-anterior pattern and a negative posterior-anterior index points towards a pattern of information flow in the opposite direction. The posterior-anterior index was also normalized by the difference between the maximum and the minimum of all observed posterior-anterior values. All observed posterior-anterior values were then tested against the null hypothesis of being significantly high or low by permuting the needed averaged directed transfer entropy values and re-calculating the posterior-anterior value (5000 repetitions).

We repeated the analysis for randomly reshuffled versions of the structural adjacency matrix. We used a reshuffling technique where we selected two matrix entries at random and then interchanged their matrix entries preserving the number of links in the network. We repeated this reshuffling step 1000 times to obtain one reshuffled version of the matrix. In the same way, we generated 100 reshuffled versions of the structural adjacency matrix. This method does not preserve the individual degrees and also not necessarily the degree distribution; it rewires our network connections ignoring any preferences for posterior or anterior regions. Thus, the links of the resulting reshuffled networks are randomly distributed and the spatial distribution of the degrees is uniformly spread over the whole network.

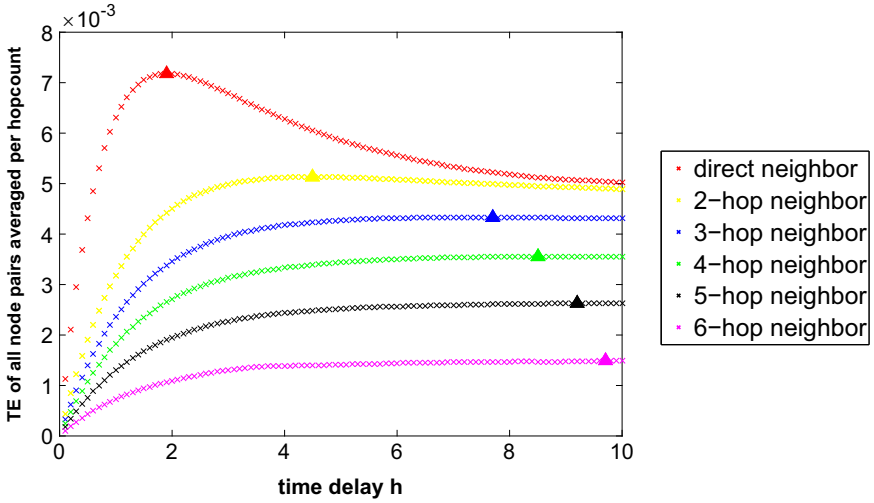

Fig. 3. Transfer entropy over different time delays. Averaged transfer entropy (TE) of all node pairs for different time delays. The transfer entropy values for different node pairs are colored differently according to the hopcount between them. We observe that direct neighbors have the highest transfer entropy and that the further apart two nodes are in terms of hopcount, the smaller the transfer entropy between them. The triangles mark the maximum transfer entropy value for each hopcount over all time delays. The larger the hopcount, the larger is the time delay needed to reach this maximum transfer entropy value.

Results

We plotted the averaged transfer entropy over all node pairs for different time delays h in Fig. 3 depending on the hopcount between them (i.e. the number of hops or links in the shortest path connecting the two nodes). The notion of a hopcount refers to the distance between two nodes (cortical regions) measured as the minimal number of links (hops) that one has to traverse in order to reach one node from the other node in the underlying structural network. We observed that a direct structural connection leads to the highest transfer entropy value between two nodes, and that the further two nodes are apart in terms of hopcount, the smaller the transfer entropy between them. For each hopcount, there exists a certain time delay h that maximizes the average transfer entropy (Fig. 3). We observed that the further another node is away (in terms of hopcount), the longer time delay is necessary to maximize the influence (transfer entropy) on that node.

Concerning the global patterns of information flow, we found three regimes depending on the chosen time delay (see Fig. 4a). For small time delays, we observed a significantly negative posterior-anterior value, i.e. an information flow from anterior to posterior regions (regime (I), P value <0.05, Fig. A.3 in Supplementary material). After a transition phase (regime (II), no significant posterior-anterior value), the opposite pattern was observed (regime (III)), i.e. a posterior-to-anterior information flow, where the posterior-anterior values for larger time delays were significantly positive (P value <0.05). In addition, depending on the time delay the structural degree correlated positively or negatively with the average directed transfer entropy (see Figs. 4b and 4c). In regime (I), we observed a significantly negative correlation between the degree and the average directed transfer entropy, which means that higher degree nodes seem to be stronger receivers of information from the network than lower degree nodes (see Fig. 4d). The significance of the correlation was tested similarly to the posterior-anterior value by permuting the directed transfer entropy values and recomputing the correlation in order to establish a null distribution (5000 repetitions, null hypothesis of observing a significantly higher or lower correlation, Fig. A.3 in Supplementary material). From a certain time delay onwards (regime (III)), the correlation between degree and directed transfer entropy became significantly positive (Fig. 4c), identifying hubs as strong senders of information. When visualizing the directed transfer entropy values on the template brain for the minimum and maximum posterior-anterior value, we recognize a global front-to-back and back-to-front pattern, respectively (see Figs. 4d and 4e). In Fig. 4d, the anterior regions seem to possess more outgoing flow of information (darker colors) and the posterior regions have a more incoming flow (lighter colors) for h=0.2, whereas the opposite pattern can be perceived for h=6 (Fig. 4e).

The results for the reshuffled version of the structural adjacency matrix with a uniform degree distribution over posterior and anterior regions show a less variant behavior for different time delays (see Appendix B in Supplementary material). For the randomly reshuffled matrices, we observe a significantly positive correlation (yet decreasing for longer time delays) between the node degree and the directed transfer entropy. However, in comparison with the structural adjacency matrix, the reshuffled matrices do not reach such high (low) correlation values for longer (shorter) time delays (see Figs. B.2 and B.3 in Supplementary material). Concerning the resulting global pattern, we observe a slightly positive posterior-anterior value for most of the randomly reshuffled matrices (see Fig. B.1 in Supplementary material). In line with the correlation values, the randomly reshuffled matrices do not show much variance over different time delays with respect to their posterior-anterior values (Figs. B.1 and B.3 in Supplementary material).

We also repeated our analysis on the directed structural macaque brain (Honey et al., 2007) (see Appendix C in Supplementary material). In this directed network, nodes possessing a high total number of connections seem to have a more sending property in general. However, for short time delays, hubs with more incoming than outgoing links, appear to be more receiving (for a detailed description see Appendix C in Supplementary material).

Discussion

Using a simple model of activity spread, we were able to reproduce the empirically observed global patterns of effective connectivity. In addition, the structural degree of a node was identified as a strong indicator for the sending/receiving property of a brain region. Moreover, the further two brain regions were away in terms of hopcount in the structural network, the smaller the transfer entropy between them.

Our study shows that the structural (topological) distance between two brain regions has an influence on their transfer entropy. From our simulation results, we can conclude that the further apart two nodes are in terms of hopcount in the underlying structural brain network, the smaller their transfer entropy. This result is in line with our previous study that identified the structural hopcount as a driving force behind functional connectivity (Meier et al., 2016). Stam et al. (2016)

(a) Posterior-anterior (PA) value and correlation between degree and average directed transfer entropy over different time delays.

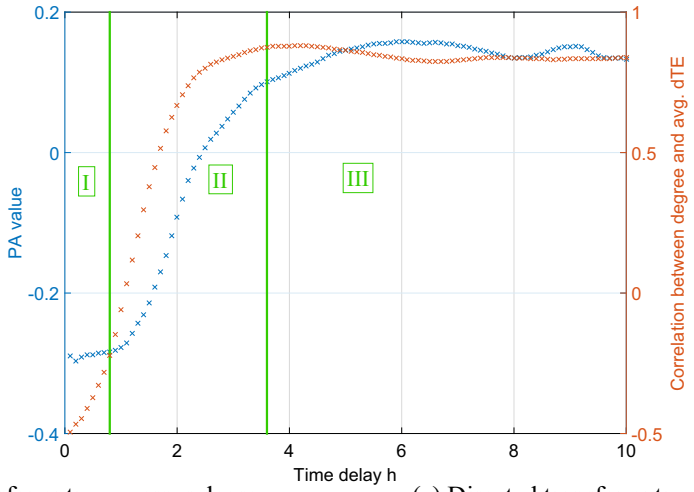

(b) Directed transfer entropy versus degree for $h = 0.2$ (regime (I)).

(c) Directed transfer entropy versus degree for $h = 6$ (regime (III)).

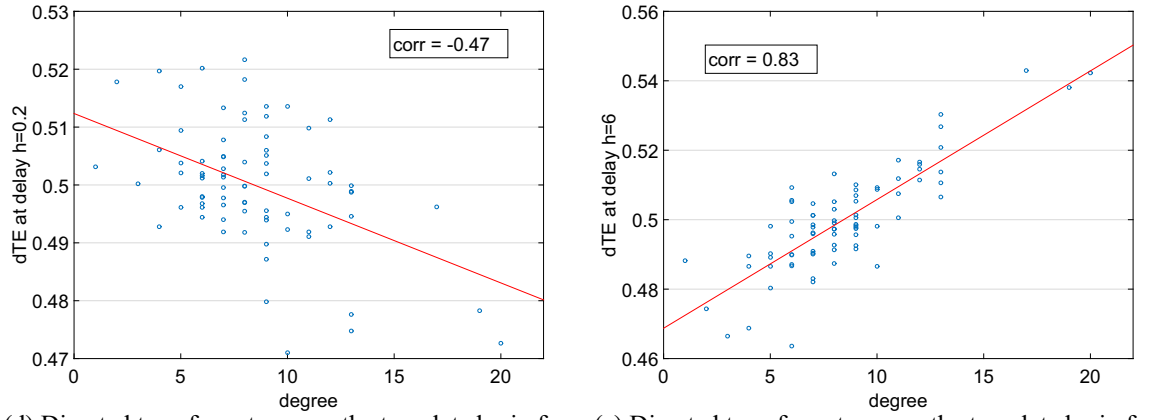

(d) Directed transfer entropy on the template brain for $h = 0.2$ (regime (I)).

(e) Directed transfer entropy on the template brain for $h = 6$ (regime (III)).

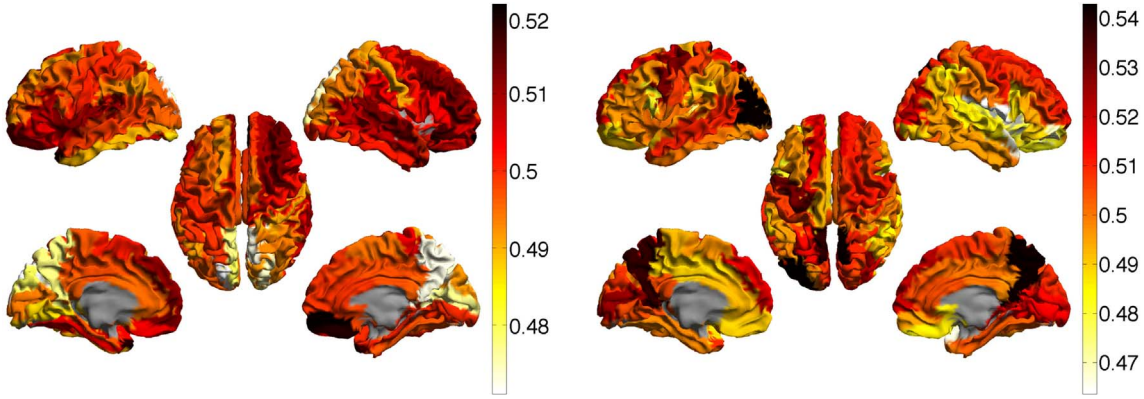

Fig. 4. Opposite patterns of information flow. (a) Posterior-anterior value and correlation between degree and averaged directed transfer entropy (dTE) over different time delays. In regime (I) we observe a significantly negative posterior-anterior value and correlation. In (II) we have a transition phase and in (III) we face a significantly positive correlation and posterior-anterior value. (b) Averaged dTE versus degree for the time delay with minimal posterior-anterior value, h=0.2. (c) Averaged dTE versus degree for the time delay with maximal posterior-anterior value, h=6. (d)+(e) dTE for each brain region on the parcellated template brain for h=0.2 (d) and h=6 (e). We show the brain here in clockwise order from the left, top, right, right midline and left midline.

found the highest effective connectivity as the result of a direct structural connection and (Honey et al., 2009) stated that indirect connections with the hopcount 2 have a strong influence on the strength of functional connections between brain regions. Moreover, Goñi et al. (2014) stated that shortest paths of the structural network and detours along them are good predictors for functional connectivity, which also implicates a lower connectivity for node pairs with larger hopcount between them. These results confirm the common assumption that longer paths in the structural brain network only have a small influence on the functional connectivity between two brain regions

(Sarkar et al., 2015; Zamora-López et al., 2016; Meier et al., 2016). Our results are in agreement with these earlier studies by identifying the hopcount between two brain regions as an indicator for their functional interaction and show that these general principles also hold for effective connectivity.

We were able to replicate the empirically observed global directionality patterns based on a simple epidemic spreading process. Without imposing any directionality on the pairwise structural interactions, we observed an overall dominant pattern of directionality based on an underlying *undirected* structural network. It therefore seems that the pure presence of an unequal degree distribution with a spatial gradient along the anterior posterior axis is enough to create overall predominant directions of information flow. The observed direction of information flow in our model depended on the chosen time delay for the estimation of the transfer entropy. The empirically discovered anterior-to-posterior pattern in lower frequency bands (*theta*) resembles the patterns observed in our model when using short time delays, whereas the opposite pattern that is empirically observed in higher frequency bands (*alpha1*, *alpha2* and *beta*) coincides with the patterns in our model when applying longer time windows (Hillebrand et al., 2016). These opposite directions of information flow probably indicate the presence of a loop between the two interacting subsystems of the Default Mode Network, the temporal and the fronto-parietal system representing a mechanism of integration of brain function (Edelman and Gally, 2013). The temporal system is involved in memory and the fronto-parietal system is responsible for self-relevant mental simulations (Buckner et al., 2008). These two processes, memory and self-relevant mental simulations, seem to be active simultaneously and on different time scales, which could provide a biological interpretation of the mirrored directions of information flow. Furthermore, these opposite directions have also been reported in invasive animal recordings, for e.g. the visual system (Van Kerkoerle et al., 2014; Bastos et al., 2015), and could represent the mechanism of memory consolidation (Sirota et al., 2008).

Our modeling results suggest that the opposite directions of the global pattern of information flow reveal the different time scales of the spreading process and seem to be linked to the sending/receiving properties of the structural hubs. For short time delays, our results show that direct neighbors influence nodes much more than indirect neighbors (Fig. 3). Stam et al. (2016) showed previously that hubs are overall more often activated (by their direct neighbors) than lower degree nodes. Because of the higher number of potentially activated direct neighbors, the activation of hubs does not only occur more frequently but also with a higher activation rate (see Eq. (1)) and thus on a shorter time scale than the activation of lower degree nodes. This frequent activation of hubs on a shorter time scale is probably the reason that hubs are strong receivers and, in return, lower degree nodes appear to be strong senders of information flow on short time scales. Since structural brain networks have the strongest hubs in posterior regions (Buckner et al., 2008), these posterior hubs acting as preferred receivers cause the anterior-posterior information flow for short time delays in our model. For longer time delays, the dominant influence of the direct neighbors decreases and the influence of the indirect neighbors increases (Fig. 3). Because hubs are activated more often and can activate not only more direct but also, on longer time scales, more indirect neighbors, they are strong senders of information for longer time scales. On the contrary, lower degree nodes have less influence on the network and act as strong receivers of information flow for longer time delays in our model. Together, these scenarios provide a possible explanation for the posterior-anterior pattern of information flow in our SIS model in the case of longer time delays. Summing up, the posterior hubs seem to play a dominant role for the global patterns, which are hypothesized to represent a mechanism of integration (Hillebrand et al., 2016). The hypothesis is further strengthened by the disappearance of the opposite information flow directions in the randomly reshuffled networks. Thus, the uneven spatial distribution of the degrees seems to be a necessary (but maybe not sufficient) condition for observing mirrored directions of global information flows. This finding is in line with multiple studies that uncover hubs to drive the integration of information in the human brain (Sporns et al., 2007) and to play a special role in both the healthy (Gong et al., 2009; Hagmann et al., 2008) and diseased brain (Crossley et al., 2014). van den Heuvel et al. (2012) have shown that a large proportion of shortest paths travels through the structural hubs. Assuming that (part of) the communication passes through shortest paths, these hubs are very likely both strong senders and receivers, which could lead to a mirrored pattern of information flow. Furthermore, a recent study by Gollo et al. (2015) concluded for the primate brain that structural hubs are “slaves” of their many connections since they not only have a powerful influence on the global network dynamics but also receive a lot of input from the rest of the network. Our results for the directed structural macaque brain confirm this different behavior for hubs regarding different time scales (see Appendix C in Supplementary material). These results provide some intuitive explanation for the opposite directions of information flow, towards the posterior hubs and, simultaneously (though on a different time scale), away from them.

Recent studies applying causality measures like transfer entropy (Hahs and Pethel, 2011) and Granger causality (Matias et al., 2014) identified a system of anticipatory synchronization as the driving force behind counterintuitive information flow directions. Anticipatory synchronization means that the receiver can learn to anticipate the sender's actions, which requires an adapting system. Hahs and Pethel (2011) have shown that in such a system the estimated role of the sender and receiver can switch depending on the applied sampling rate. The simple SIS model does not allow anticipation and the described phenomenon caused by anticipatory synchronization can thus not apply to the modeling results. However, the dynamics of anticipation have already been reported for empirical brain dynamics (Leaver et al., 2009) and for task-related data of the macaque brain (Matias et al., 2014). Thus, for empirical observations of counterintuitive directions of information flow, the sampling rate (Hahs and Pethel, 2011) could indeed provide an explanation.

We applied a simple SIS epidemic spreading model that ignored microscopic details of the real underlying neuronal processes in order to analyze global patterns. Even though our model ignored heterogeneity except for the underlying structural network restrictions, we were able to generate the empirically found global, directed spreading patterns (Hillebrand et al., 2016). The SIS model can be regarded as a simplified version of the neural transmission dynamics, which deliberately ignores microscopic details of the underlying neural dynamics and neuronal architecture in order to allow macroscopic whole-brain analysis. This type of model is “conceptual”: the aim is not to explain neurons, spikes, synapses etc., but the topology of large-scale brain networks and their global network dynamics. Our approach aligns with other recent studies analyzing global spreading dynamic principles with the help of simple dynamic models (Mišić et al., 2015; Tagliazucchi et al., 2016). Mišić et al. (2015) found, applying a deterministic cascade model, that the hubs and a backbone of core pathways facilitate the spreading process and shortest paths accelerate this phenomenon. Similarly, diffusion models have identified the shortest path structure of the structural brain network as a driving force behind the network dynamics (Goñi et al., 2014) and categorized functional modules of the brain (Betzel et al., 2013; Delvenne et al., 2010). These simple modeling approaches should be considered as complementary to the traditional neural mass and field models from computational neuroscience (Deco et al., 2008). Most importantly, these simpler models allow us to study the basic principles of dynamics on brain networks with a minimum set of a-priori assumptions and parameters. For more complex models, the emergence of any global pattern could be ascribed to any of the (many) underlying model properties. In our case, because of the simplicity of the model and the

underlying undirected network, the emergence of global patterns of effective connectivity can be traced back to the spatially unequal distribution of hubs.

Conclusion

In this study, we analyzed local and global network dynamics of the brain network by applying an SIS epidemic spreading model on the human connectome. We found that direct structural connections induced higher transfer entropy between two brain regions and that transfer entropy decreased with increasing distance between nodes (in terms of hops in the structural network). Applying the SIS model, we were able to confirm the empirically observed information flow patterns based on an underlying *undirected* structural network where posterior hubs seem to play a dominant role in the network dynamics. For small time scales, when these hubs acted as strong receivers of information, the global pattern of information flow was in the posterior-to-anterior direction and in the opposite direction when they were strong senders. Our analysis suggests that these global patterns of directional information flow are the result of an unequal spatial distribution of the structural degree between posterior and anterior regions and the direction of information flow seem to be linked to different time scales of the spreading process. Based on the developed framework, future studies should investigate how structural changes in patients suffering from brain disorders can influence these global patterns of information flow.

Acknowledgments

We thank Gaolang Gong for providing structural network data. Further, we thank Ruud van de Bovenkamp for his useful comments and for making his SIS simulator available to us.

Appendix A. Supplementary material

Supplementary data associated with this article can be found in the online version at http://dx.doi.org/10.1016/j.neuroimage.2017.02.007.

References

Abdelnour, F., Voss, H.U., Raj, A., 2014. Network diffusion accurately models the relationship between structural and functional brain connectivity networks. NeuroImage 90, 335–347.
Aertsen, A., Gerstein, G., Habib, M., Palm, G., 1989. Dynamics of neuronal firing correlation: modulation of effective connectivity. J. Neurophysiol. 61 (5), 900–917.
Bastos, A.M., Vezoli, J., Bosman, C.A., Schoffelen, J.-M., Oostenveld, R., Dowdall, J.R., de Weerd, P., Kennedy, H., Fries, P., 2015. Visual areas exert feedforward and feedback influences through distinct frequency channels. Neuron 85 (2), 390–401.
Betzel, R.F., Griffa, A., Avena-Koenigsberger, A., Goñi, J., Thiran, J.-P., Hagmann, P., Sporns, O., 2013. Multi-scale community organization of the human structural connectome and its relationship with resting-state functional connectivity. Netw. Sci. 1 (03), 353–373.
Buckner, R.L., Andrews-Hanna, J.R., Schacter, D.L., 2008. The brain's default network. Ann. N.Y. Acad. Sci. 1124 (1), 1–38.
Bullmore, E., Sporns, O., 2012. The economy of brain network organization. Nat. Rev. Neurosci. 13 (5), 336–349.
Cator, E., van Mieghem, P., 2013. Susceptible-infected-susceptible epidemics on the complete graph and the star graph: exact analysis. Phys. Rev. E 87 (1), 012811.
Crossley, N.A., Mechelli, A., Scott, J., Carletti, F., Fox, P.T., McGuire, P., Bullmore, E.T., 2014. The hubs of the human connectome are generally implicated in the anatomy of brain disorders. Brain 137 (8), 2382–2395.
Dauwan, M., van Dellen, E., van Boxtel, L., van Straaten, E.C., de Waal, H., Lemstra, A.W., Gouw, A.A., van der Flier, W.M., Scheltens, P., Sommer, I.E., et al., 2016. EEG-directed connectivity from posterior brain regions is decreased in dementia with lewy bodies: a comparison with Alzheimer's disease and controls. Neurobiol. Aging 41, 122–129.
de Haan, W., Mott, K., van Straaten, E.C., Scheltens, P., Stam, C.J., 2012. Activity dependent degeneration explains hub vulnerability in Alzheimer's disease. PLoS Comput. Biol. 8 (8), e1002582.
Deco, G., Jirsa, V.K., Robinson, P.A., Breakspear, M., Friston, K., 2008. The dynamic brain: from spiking neurons to neural masses and cortical fields. PLoS Comput. Biol. 4 (8), e1000092.
Deco, G., Senden, M., Jirsa, V., 2012. How anatomy shapes dynamics: a semi-analytical study of the brain at rest by a simple spin model. Front. Comput. Neurosci., 6.
Delvenne, J.-C., Yaliraki, S.N., Barahona, M., 2010. Stability of graph communities across time scales. Proc. Natl. Acad. Sci. 107 (29), 12755–12760.
Edelman, G.M., Gally, J.A., 2013. Reentry: a key mechanism for integration of brain function. Front. Integr. Neurosci., 7.
Friston, K.J., 1994. Functional and effective connectivity in neuroimaging: a synthesis. Hum. Brain Mapp. 2 (1–2), 56–78.
Gollo, L.L., Zalesky, A., Hutchison, R.M., van den Heuvel, M., Breakspear, M., 2015. Dwelling quietly in the rich club: brain network determinants of slow cortical fluctuations. Philos. Trans. R. Soc. B 370 (1668), 20140165.
Gong, G., He, Y., Concha, L., Lebel, C., Gross, D.W., Evans, A.C., Beaulieu, C., 2009. Mapping anatomical connectivity patterns of human cerebral cortex using in vivo diffusion tensor imaging tractography. Cereb. Cortex 19 (3), 524–536.
Goñi, J., van den Heuvel, M.P., Avena-Koenigsberger, A., de Mendizabal, N.V., Betzel, R.F., Griffa, A., Hagmann, P., Corominas-Murtra, B., Thiran, J.-P., Sporns, O., 2014. Resting-brain functional connectivity predicted by analytic measures of network communication. Proc. Natl. Acad. Sci. 111 (2), 833–838.
Hagmann, P., Cammoun, L., Gigandet, X., Meuli, R., Honey, C.J., Wedeen, V.J., Sporns, O., 2008. Mapping the structural core of human cerebral cortex. PLoS Biol. 6 (7), e159.
Hahs, D.W., Pethel, S.D., 2011. Distinguishing anticipation from causality: anticipatory bias in the estimation of information flow. Phys. Rev. Lett. 107 (12), 128701.
Haimovici, A., Tagliazucchi, E., Balenzuela, P., Chialvo, D.R., 2013. Brain organization into resting state networks emerges at criticality on a model of the human connectome. Phys. Rev. Lett. 110 (17), 178101.
Hillebrand, A., Tewarie, P., van Dellen, E., Yu, M., Carbo, E.W., Douw, L., Gouw, A.A., van Straaten, E.C., Stam, C.J., 2016. Direction of information flow in large-scale resting-state networks is frequency-dependent. Proc. Natl. Acad. Sci. 113 (14), 3867–3872.
Honey, C., Sporns, O., Cammoun, L., Gigandet, X., Thiran, J.-P., Meuli, R., Hagmann, P., 2009. Predicting human resting-state functional connectivity from structural connectivity. Proc. Natl. Acad. Sci. 106 (6), 2035–2040.
Honey, C.J., Kötter, R., Breakspear, M., Sporns, O., 2007. Network structure of cerebral cortex shapes functional connectivity on multiple time scales. Proc. Natl. Acad. Sci. 104 (24), 10240–10245.
Leaver, A.M., van Lare, J., Zielinski, B., Halpern, A.R., Rauschecker, J.P., 2009. Brain activation during anticipation of sound sequences. J. Neurosci. 29 (8), 2477–2485.
Liu, Q., Van Mieghem, P., 2016a. Die-out probability in SIS epidemic processes on networks. In: International Workshop on Complex Networks and their Applications, Springer, pp. 511–521.
Liu, Q., Van Mieghem, P., 2017. Evaluation of an analytic, approximate formula for the time-varying SIS prevalence in different networks. Physica A 471, 325–336.
Lobier, M., Siebenhühner, F., Palva, S., Palva, J.M., 2014. Phase transfer entropy: a novel phase-based measure for directed connectivity in networks coupled by oscillatory interactions. NeuroImage 85, 853–872.
Matias, F.S., Gollo, L.L., Carelli, P.V., Bressler, S.L., Copelli, M., Mirasso, C.R., 2014. Modeling positive Granger causality and negative phase lag between cortical areas. NeuroImage 99, 411–418.
Meier, J., Tewarie, P., Hillebrand, A., Douw, L., van Dijk, B.W., Stufflebeam, S.M., Van Mieghem, P., 2016. A mapping between structural and functional brain networks. Brain Connect. 6 (4), 298–311.
Mišić, B., Betzel, R.F., Nematzadeh, A., Goñi, J., Griffa, A., Hagmann, P., Flammini, A., Ahn, Y.-Y., Sporns, O., 2015. Cooperative and competitive spreading dynamics on the human connectome. Neuron 86 (6), 1518–1529.
Moon, J.-Y., Lee, U., Blain-Moraes, S., Mashour, G.A., 2015. General relationship of global topology, local dynamics, and directionality in large-scale brain networks. PLoS Comput. Biol. 11 (4), e1004225.
Paluš, M., Stefanovska, A., 2003. Direction of coupling from phases of interacting oscillators: an information-theoretic approach. Phys. Rev. E 67 (5), 055201.
Pastor-Satorras, R., Castellano, C., Van Mieghem, P., Vespignani, A., 2015. Epidemic processes in complex networks. Rev. Mod. Phys. 87 (3), 925.
Rubinov, M., Sporns, O., Thivierge, J.-P., Breakspear, M., 2011. Neurobiologically realistic determinants of self-organized criticality in networks of spiking neurons. PLoS Comput. Biol. 7 (6), e1002038.
Sarkar, S., Chawla, S., Xu, D., 2015. On inferring structural connectivity from brain functional-MRI data. arXiv preprint arXiv:1502.06659.
Schreiber, T., 2000. Measuring information transfer. Phys. Rev. Lett. 85 (2), 461.
Sirota, A., Montgomery, S., Fujisawa, S., Isomura, Y., Zugaro, M., Buzsáki, G., 2008. Entrainment of neocortical neurons and gamma oscillations by the hippocampal theta rhythm. Neuron 60 (4), 683–697.
Sporns, O., Honey, C.J., Kötter, R., 2007. Identification and classification of hubs in brain networks. PLoS One 2 (10), e1049.
Stam, C.J., 2014. Modern network science of neurological disorders. Nat. Rev. Neurosci. 15 (10), 683–695.
Stam, C.J., Hillebrand, A., van Dellen, E., Meier, J., Tewarie, P., van Straaten, E., Van Mieghem, P., 2016. The relation between structural and functional connectivity patterns in complex brain networks. Int. J. Psychophysiol. 103, 149–160.
Stam, C.J., Van Straaten, E., 2012. The organization of physiological brain networks. Clin. Neurophysiol. 123 (6), 1067–1087.
Stam, C.J., van Straaten, E.C., 2012. Go with the flow: use of a directed phase lag index (dPLI) to characterize patterns of phase relations in a large-scale model of brain dynamics. NeuroImage 62 (3), 1415–1428.
Tagliazucchi, E., Chialvo, D.R., Siniatchkin, M., Amico, E., Brichant, J.-F., Bonhomme, V., Noirhomme, Q., Laufs, H., Laureys, S., 2016. Large-scale signatures of unconsciousness are consistent with a departure from critical dynamics. J. R. Soc.

Interface 13 (114), 20151027.
Tewarie, P., Hillebrand, A., van Dellen, E., Schoonheim, M., Barkhof, F., Polman, C., Beaulieu, C., Gong, G., van Dijk, B., Stam, C., 2014. Structural degree predicts functional network connectivity: a multimodal resting-state fMRI and MEG study. NeuroImage 97, 296–307.
Tewarie, P., Hillebrand, A., van Dijk, B.W., Stam, C.J., O'Neill, G.C., Van Mieghem, P., Meier, J.M., Woolrich, M.W., Morris, P.G., Brookes, M.J., 2016. Integrating cross-frequency and within band functional networks in resting-state MEG: a multi-layer network approach. NeuroImage.
Tzourio-Mazoyer, N., Landeau, B., Papathanassiou, D., Crivello, F., Etard, O., Delcroix, N., Mazoyer, B., Joliot, M., 2002. Automated anatomical labeling of activations in spm using a macroscopic anatomical parcellation of the mni mri single-subject brain. NeuroImage 15 (1), 273–289.
van de Bovenkamp, R., 2015. Epidemic Processes on Complex Networks: Modelling, Simulation and Algorithms. (Ph.D. thesis), TU Delft.
van den Heuvel, M.P., Kahn, R.S., Goñi, J., Sporns, O., 2012. High-cost, high-capacity backbone for global brain communication. Proc. Natl. Acad. Sci. 109 (28), 11372–11377.
Van Kerkoerle, T., Self, M.W., Dagnino, B., Gariel-Mathis, M.-A., Poort, J., Van Der Togt, C., Roelfsema, P.R., 2014. Alpha and gamma oscillations characterize feedback and feedforward processing in monkey visual cortex. Proc. Natl. Acad. Sci. 111 (40), 14332–14341.
Van Mieghem, P., 2014b. Performance Analysis of Complex Networks and Systems. Cambridge University Press, Cambridge, United Kingdom.
Wiener, N., 1956. The theory of prediction. Mod. Math. Eng. 1, 125–139.
Yu, S., Yang, H., Shriki, O., Plenz, D., 2013. Universal organization of resting brain activity at the thermodynamic critical point. Front. Syst. Neurosci., 7.
Zamora-López, G., Chen, Y., Deco, G., Kringelbach, M.L., Zhou, C., 2016. Functional Complexity Emerging from Anatomical Constraints in the Brain: The Significance of Network Modularity and Rich-clubs, arXiv preprint arXiv:1602.07625.